Hand Vein Recognition Based on Oriented Gradient Maps and Local Feature Matching

Di Huang[1], Yinhang Tang[1], Yiding Wang[2], Liming Chen[3], and Yunhong Wang[1]

[1] Laboratory of Intelligence Recognition and Image Processing, School of Computer Science and Engineering, Beihang University, Beijing 100191, China
[2] College of Info. Eng., North China University of Technology, Beijing, 100041, China
[3] Université de Lyon, CNRS, Ecole Centrale Lyon, LIRIS, Lyon, 69134, France

Abstract. The hand vein pattern as a biometric trait for identification has attracted increasing interests in recent years thanks to its properties of uniqueness, permanence, non-invasiveness as well as strong immunity against forgery. In this paper, we propose a novel approach for back of the hand vein recognition. It first makes use of Oriented Gradient Maps (OGMs) to represent the Near-Infrared (NIR) hand vein images, simultaneously highlighting the distinctiveness of vein patterns and texture of their surrounding corium, in contrast to the state-of-the-art studies that only focused on the segmented vein region. SIFT based local matching is then performed to associate the keypoints between corresponding OGM pairs of the same subject. The proposed approach was benchmarked on the NCUT database consisting of 2040 NIR hand vein images from 102 subjects. The experimental results clearly demonstrate the effectiveness of our approach.

1 Introduction

Driven mainly by an increasing requirement for security against terrorist activities, sophisticated crimes, as well as electronic frauds, biometric based solutions have witnessed an accelerated pace of growth in the global market of security over the last several decades. Recently, a new biometric, named hand veins, has emerged for the purpose of people identification.

Anatomically, the veins are the blood carrying vessels interweaved with muscles and bones, and the fundamental function of the vascular system is to supply oxygen to each part of the body. The spatial arrangement of the vascular network in human body is quite stable and unique, and vein patterns of individuals are different, even between identical twins [1]. In this work, we concentrate on the vein patterns of back of the hand since they are distinctly visible, easy to acquire, and efficient to process. As compared with other popular biometric traits, like face or fingerprint, hand vein patterns possess several main merits, in particular the following ones:

- Direct liveness test. As hand veins are imaged by using far or near infrared lighting to capture temperature differences between the flow of hot blood in the

K.M. Lee et al. (Eds.): ACCV 2012, Part IV, LNCS 7727, pp. 430–444, 2013.

veins and surrounding skin, they can only be imaged on live body and the images taken on non-live bodies cannot capture their spatial vein arrangement;

- Safety. Blood vessel patterns are hardwired underneath the skin at birth; they are hence much harder for intruders to forge.

Vein pattern as biometric trait is relatively recent. It was not exploited until 1990 when MacGregor and Welford [2] came up with their system called vein check for people identification. Despite the vast vascular network in human body, hand veins are largely favored for their simplicity in processing and there exists an increasing amount of work in the last decade, using hand vein patterns of the palm part [3,4], back of the hand [5,6,7] or finger veins [8] (refer to the standard ISO/IEC 19794-9 for more detailed definitions of different hand vein patterns).

Most tasks in the literature followed the framework that first segments the region of interest and hand subcutaneous vascular network from hand vein images, and then extracts local geometric features for matching, such as the positions and angles of short straight vectors [9], endpoints and crossing points [10], dominant points [5], vein minutiae and knuckle shape [7]. All these methods demonstrate reasonable recognition accuracies on small databases ranging from 32 [5] to 100 subjects [1,7], however, when regarding the problem of back of the hand vein recognition, the above techniques suffer from limited local features because compared with the palm and finger part, the number of vein minutiae on the back of the hand is really few, leading to a deficiency in capturing differences of vein networks between subjects. Meanwhile, NIR imaging systems deliver vein patterns along with the surrounding texture of corium in the same image, but the texture information of corium is rarely used. Intuitively, if its details can be highlighted, there should be distinctive cues for improved performance.

In this paper, we propose a novel approach for back of the hand vein recognition. It adopts Oriented Gradient Maps (OGMs) originally proposed to describe 3D face models (i.e. range and texture images) under the term of Perceived Facial Images (PFIs) [11], to represent hand vein images, simultaneously highlighting the distinctiveness of the vascular pattern as well as the texture of its surrounding corium. Using these OGMs instead of the original raw hand vein images, SIFT-based local matching is then carried out to associate local features between the backs of two hands, and to account for slight geometrical transformations (e.g. rotations, translations) and possible lighting variations (NIR intensity changes) that can occur on hand vein images. The proposed method was benchmarked on Near Infrared (NIR) hand-dorsa vein images in NCUT, one of the largest hand vein databases so far known in the literature, consisting of 2040 right and left hand-dorsa vein images of 102 subjects. The achieved experimental result clearly demonstrates the effectiveness of the proposed approach.

2 NIR Vein Image Acquisition

Hand veins can be imaged either by Far-Infrared (FIR) or Near-Infrared (NIR) imaging techniques, thereby providing a manner of contactless and non-invasive data acquisition. Wang and Leedham [12] made a study in depth to compare

FIR and NIR imaging techniques for vein pattern biometrics, and concluded that FIR imaging techniques are sensitive to ambient conditions such as temperature, humidity and human body condition, and hence do not deliver a stable quality. Meanwhile, they pointed out that NIR imaging techniques produce good quality images that are tolerant to variations in environmental and body condition. In this work, back of the hand vein images were sensed by a NIR imaging system developed by Wang et al. [13,14].

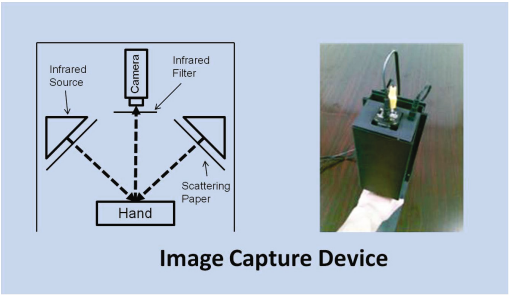

Fig. 1. The setup of the NIR imaging system

Fig.1 illustrates the system setup where an LED array lamp is utilized to shine infrared light onto the back of the hand. Because the incident infrared light can penetrate into the biological tissue with an approximate depth of 3mm and venous blood generally absorbs and scatters more incident infrared radiation than surrounding tissue, vein patterns can be imaged by a CCD camera attached an IR filter where vein appears darker. In order to avoid the major hand vein image registration issue, a handle is pre-mounted at the bottom of the device to position the hand. The hand vein images are hence roughly aligned, but still differ by slight translations and rotations. Fig.2 shows a back of the hand vein image captured with a resolution of 640 by 480.

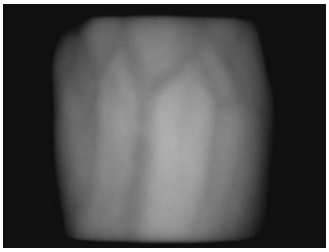

Fig. 2. A back of the hand vein image

Using this setup, a dataset of 2040 hand vein images was acquired under the natural lighting condition (indoor office environment) [6]. It was named as North

China University of Technology hand-dorsa vein database or NCUT dataset for short. In detail, 10 right and 10 left back of the hand vein images were captured from all 102 subjects, aged from 18 to 29, of which 50 were male while 52 were female. It makes the dataset one of the largest ones for hand vein biometrics. As the vein pattern is best defined when the skin on the back of the hand is taut, subjects were asked to clench their fists as acquiring vein patterns. There were no major illumination variations, but slight lighting changes still can occur since the vein images were acquired at different time.

As we can see from Fig.2, major hand vein patterns are captured and appear darker within the NIR image. Widths of these vein profiles vary in the range of 30 to 50 pixels. Even though the vein spatial arrangements are visible, they are not so distinguishable from the bio-tissue background. Moreover, local features, in terms of endpoints and crossing points, are limited and usually vary from 5 to 10, thus making local feature-based approach questionable for their ability of discriminative power. On the other hand, Fig. 2 delivers vein patterns along with the surrounding texture of corium, but the usefulness of texture information of corium is rarely investigated. Intuitively, the corium region contains critical cues for identification tasks as well, and if its details can be sufficiently highlighted, the performance of hand vein recognition could be improved.

3 Oriented Gradient Maps (OGMs)

In order to simultaneously increase the distinctiveness of the vein region as well as the texture of its surrounding corium, we propose a novel method to represent hand vein images, which makes use of Oriented Gradient Maps (OGM), originally applied to describe texture and range information in 3D face recognition [11].

The objective of OGM is to provide a visual description simulating the human visual perception and such a concept was inspired by the study of Edelman et al. [15], who proposed a representation of complex neurons in the primary visual cortex. These complex neurons respond to a gradient at a particular orientation and spatial frequency, but the location of the gradient is allowed to shift over a small receptive field rather than being precisely localized.

3.1 Representation of Complex Neuron Response

The proposed representation aims at simulating the response of complex neurons and it is based on a convolution of gradients in specific directions in a pre-defined neighborhood. Since veins of different hands have a diversity of patterns, in this study, for process simplicity, we just make use of a circular neighborhood R, as illustrated in Fig.3. The precise radius value of the circular area needs to be fixed experimentally. The response of a complex neuron at a certain pixel location is a set of gradient maps in different orientations convolved with a Gaussian kernel.

Specifically, given an input image I, a certain number of gradient maps G_1, G_2, ..., G_o, one for each quantized direction o, are firstly computed. They are defined as:

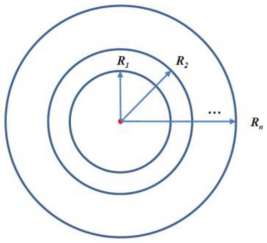

Fig. 3. The neighborhood of the complex neurons is a circular region; its radius can be changed according to the scale

$$G_o = \left(\frac{\partial I}{\partial o}\right)^+ \tag{1}$$

The "+" sign means that only positive values are kept to preserve the polarity of the intensity changes, while the negative ones are set to zero.

Each gradient map describes gradient norms of the input original image in an orientation o at every pixel. We then simulate the response of complex neurons by convolving its gradient maps with a Gaussian kernel G. The standard deviation of G is proportional to the value of radius of the given neighborhood area, R, as in eq. 2.

$$\rho_o^R = G_R * G_o \tag{2}$$

The purpose of the convolution with Gaussian kernels is to allow the gradients to shift in a neighborhood without abrupt changes.

At a given pixel location (x, y), we collect all values of the convolved gradient maps at that location and form the vector $\rho^R(x, y)$, and it thus has a response value of complex neurons for each orientation o.

$$\rho^R(x, y) = \left[\rho_1^R(x, y),\ \cdots,\ \rho_O^R(x, y)\right]^t \tag{3}$$

This vector, $\rho^R(x, y)$, is further normalized to unit norm vector, which is called response vector and denoted by $\underline{\rho}^R$.

3.2 Oriented Gradient Maps by Response Vectors

According to the response vectors, an image can be represented by its perceived values of complex neurons. In this work, the original input image is NIR back of the hand vein image. Specifically, given a raw image I, we generate an Oriented Gradient Map (OGM) J_o using complex neurons for each orientation o defined as in eq. 4.

$$J_o(x, y) = \underline{\rho}_o^R(x, y) \tag{4}$$

Fig.4 depicts such a process applied to a NIR back of the hand vein image. In our work, we generate eight OGMs for eight pre-defined quantized directions. Instead of original NIR back of the hand images, these OGMs are thus used for the subsequent matching for hand vein identification.

3.3 The Properties of Distinctiveness and Invariance

The OGMs potentially offer high distinctiveness as they highlight the details of local texture variations. Meanwhile, they also possess some interesting properties of robustness to affine lighting variations

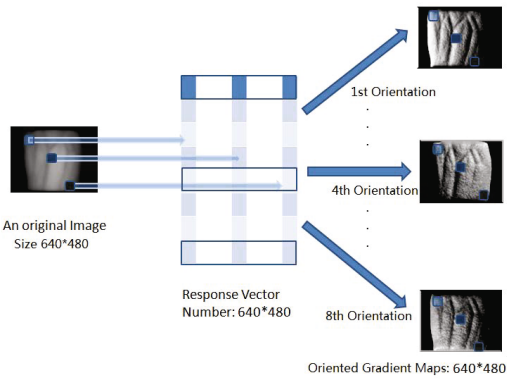

Fig. 4. The OGMs describe a perceived NIR hand vein image in 8 orientations

When applied OGMs to 2D texture images, e.g. NIR back of the hand images, it offers the property of being robust to affine illumination transformations. Indeed, an OGM J_o is simply normalized convolved gradient maps at the orientation o, while monotonic illumination changes often adds a constant intensity value, as a result, it does not affect the computation of gradients. Furthermore, a change in image contrast in which the intensities of all the pixels are multiplied by a constant will lead to the multiplication of gradient computation; however, this contrast change will be cancelled by the normalization of response vectors.

OGMs can be made even rotation invariant if we chose to quantize directions starting from the principal gradient direction of all the gradients within a given neighborhood. Nevertheless, we do not perform such rotation normalization for saving computational cost as NIR back of the hand vein images in NCUT were already roughly aligned.

3.4 Difference Discussion with the State of the Art

In the literature, a few Gaussian filter based descriptors also exist, such as Gabor filter [16] and Daisy descriptor [17]. Gabor filters, which are spatially localized and selective to spatial orientations and scales, are comparable to the receptive

fields of simple cells in mammalian visual cortex [18]. Whilst the Daisy descriptor convolves these gradient maps of pre-defined directions with Gaussian filters of different kernel sizes arranged based on a daisy-style neighborhood to compose a comprehensive representation of an image.

Compared with the two descriptors mentioned above, i.e. Gabor filters and daisy, the proposed OGMs fundamentally share the same biological vision principal to build complex neurons for image representation. Considering that the input image required by the following keypoint detection should have sufficient details, to only highlight the distinctiveness of these hand vein images and avoid the very smooth results given by larger Gaussian kernels, we experimentally set the radius of the circular neighborhood at a specific value rather than introduce the multi-scale strategy as applied by Daugman [19], which computes average gradient variations between adjacent circular rings according to a coarse-to-fine scheme supported by varying kernel based Gaussian smoothing. As a result, the computation of the OGMs is more efficient.

Finally, the OGMs are a set of output images whose details are greatly enhanced with all preserved spatial information (see Fig.4), which is suitable for the subsequent framework of local matching and distinct from the feature vector based one as in [20].

4 Local Feature Matching

The local feature extraction directly on original hand vein images leads to few local features with low distinctiveness. On the other hand, the OGMs of a hand vein image contain much more details of local texture variations, thus simultaneously enhancing the distinctiveness of the vascular network and surrounding corium. Once OGMs of hand vein images are generated, we extract the widely-used SIFT features [21] to associates keypoints between two hand images and to account for the changes in rotation and lighting conditions. These local features are further employed for similarity score computation and final decision making.

4.1 Keypoint Detection

SIFT applies the scale-space Difference-of-Gaussian (DoG) to detect keypoints in images. A given image is repeatedly convolved with Gaussians of different scales separated by a constant factor k to produce an octave in scale space. As for an original input image, $I(x, y)$, its scale space is defined as a function, $L(x, y, \sigma)$, produced by convolution of a variable scale Gaussian $G(x, y, \sigma)$ with the image I, and the DoG function $D(x, y, \sigma)$ can be computed from the difference of two nearby scales:

$$D(x, y, \sigma) = (G(x, y, k\sigma) - G(x, y, \sigma)) * I(x, y) = L(x, y, k\sigma) - L(x, y, \sigma) \quad (5)$$

The extrema of $D(x, y, \sigma)$ can be detected by comparing each pixel value to those of its 26 neighbors within a 3×3 area at current and adjacent scales. At

each scale, gradient magnitude, $m(x, y)$, and orientation, $\theta(x, y)$, is computed by using pixel differences in eq.6 and eq.7.

$$m(x,y) = \sqrt{(L(x+1,y) - L(x-1,y))^2 + (L(x,y+1) - L(x,y-1))^2} \quad (6)$$

$$\theta(x,y) = \tanh(L(x,y+1) - L(x,y-1))/(L(x+1,y) - L(x-1,y)) \quad (7)$$

For each detected keypoint, a feature vector is extracted as a descriptor from the gradients of sampling points within its neighborhood. In order to achieve orientation invariance, coordinates and gradient orientations of sampling points in the neighborhood are rotated relative to keypoint orientation. Then a Gaussian function is used to assign a weight to gradient magnitude of each point. Points close to the keypoint are given more emphasis than the ones far from it (see [21] for more details of SIFT parameter setting). The orientation histograms of 4×4 sampling regions are calculated, each with eight orientation bins. Thus a feature vector with a dimension of 128 ($4 \times 4 \times 8$) is produced.

SIFT operates on each OGM separately. Because OGMs highlight local texture characteristics of hand vein images, much more keypoints are detected for the following SIFT matching step than those in the original NIR images. Some statistical work was done along with the experiments on the NCUT database. The number of keypoints extracted from each of OGM can rise up to 627, while that from the original hand vein image can be as few as 4. Fig.5 illustrates this phenomenon.

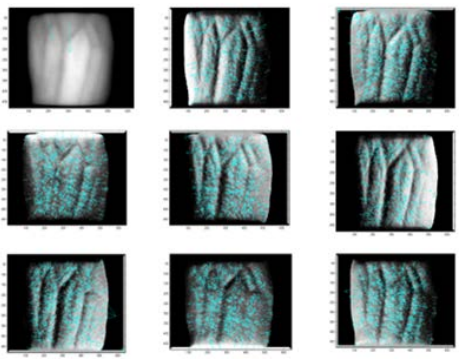

Fig. 5. SIFT-based keypoint detection. The upper row displays the original hand vein image along with the OGMs in the first two directions. The two bottom rows display the OGMs in the left six directions. All images are with their detected keypoints.

4.2 SIFT-Based Local Feature Matching

Given these local features extracted from each OGM pair of the gallery and probe hand vein images respectively, two sets of hand vein keypoints can be matched. Matching one keypoint to another is accepted only if similarity distance is less than a predefined threshold t times the distance to the second closest match. In this work, t is empirically set at 0.6 as in [21]. We can hence denote the number of the matched keypoints by N_o in an OGM pair in the the o_{th} direction. The bigger N_o is the more likely the underlying hand vein images are the same.

This similarity measure, N_o, is with a positive polarity (a bigger value means a better matching relationship). A hand vein image in the probe set is matched with every hand vein images in the gallery set. The nth element in each matching score vector corresponds to the similarity measure between the probe and the n_{th} gallery hand vein image. Each vector is normalized to the interval of [0, 1] by using the max-min rule. In order to achieve complete analysis, the matching scores of OGM pairs in all orientations are fused using a basic weighted sum rule:

$$S = \sum_{i=1}^{o} w_i \cdot N_i \tag{8}$$

The corresponding weight w_i is calculated dynamically during the online step using the scheme as in [22]:

$$w_i = \frac{\max_1(N_i) - mean(N_i)}{\max_2(N_i) - mean(N_i)} \tag{9}$$

where the operators $max_1(S)$ and $max_2(S)$ produce the first and second maximum value of the score S respectively. The gallery hand vein image which owns the maximum value is declared as the identity of the probe hand vein image.

5 Experimental Results

To comprehensively evaluate the proposed method, we designed 4 experiments that are detailedly introduced in the following subsections. The experiments were conducted in the scenario of identification as in the state-of-the-art tasks using the NCUT database described in section 2. Recall that this dataset is one of the largest datasets on NIR back of the hand vein images as it contains 10 right and 10 left hand vein images respectively for each of the 102 subjects enrolled, thus making up a dataset of 2040 hand vein images. All the hand vein images are roughly aligned thanks to the hardware configuration, but they still have slight rotation and lighting variations.

5.1 The Discriminative Power of OGMs

As it was found out that the hand vein pattern is unique to some level for each person as well as each hand [23], we hence considered three different experimental setups, namely, i) left hand vein images only, ii) right hand vein images only, iii) both the left and right hand vein images but as if we had 204 subjects each of which has 10 vein images in the dataset. For each setup, we followed a popular protocol that the first 5 images were used in the gallery set while the remaining 5 images were exploited as probes. We computed the recognition rate of each OGM and their combination as displayed in Table 1.

Table 1. Performance of each OGM and their combination in the setup of left-hand only, right-hand only and both-hands on the NCUT database

Directions	Left Hand Only	Right Hand Only	Both Hands
OGM-1	92.94%	93.53%	93.04%
OGM-2	81.18%	79.41%	78.53%
OGM-3	75.88%	77.45%	75.10%
OGM-4	73.14%	60.78%	66.18%
OGM-5	97.57%	92.55%	91.57%
OGM-6	78.82%	74.90%	75.49%
OGM-7	77.65%	84.51%	80.69%
OGM-8	78.63%	82.16%	78.82%
Fusion	99.02%	99.02%	99.02%

As we discussed in section 4, each hand vein image has very limited number of keypoints if applying DoG directly on original images, and a reasonable accuracy cannot be achieved, which concludes the fact that enhancing the distinctiveness of hand vein images by OGMs is a necessity because each OGM contributes to identification. From Table.1 we can see that the fusion of all 8 OGMs leads to a much better result than any of the single one. This fact accords with our preliminary study for this issue adopting subspace techniques [24]. Unfortunately, in that work, due to the sensitivity of holistic approaches to NIR intensity changes and hand geometric transformations, only about 70%-80% rank-one recognition rates were reported even with a easier experimental setting, and it is not accurate enough for a biometric system. On the other hand, we compared the results in the three columns, and found out that the performance only using left hand images was comparable to that only using right hand ones. When left and right hand vein images were both used and considered as captured from different subjects, the result generally remains stable, suggesting that our method works well as the class size is doubled.

5.2 The Impact of Gallery Size

Many efforts have been focused on how to improve the system accuracy, however, it seems that most of them neglect the potential problem which may stem from

the hand vein database where there are only limited sample images per person enrolled, possibly due to the difficulties of sample collection or the bottleneck of storage capability of the systems. Therefore, we vary the size of gallery samples of each person from 1 to 9 (since at least 1 sample per person should be used in the probe set) to analyze the impact of the gallery size to the proposed method, using the third protocol of both hand images defined in the last experiment. As illustrated in Fig. 6, we can see that the accuracies of each single OGM as well as their combination are generally improved as the gallery size increases, and our method can even achieve a recognition rate of 91.67% when only 2 samples are enrolled in the gallery set of each subject.

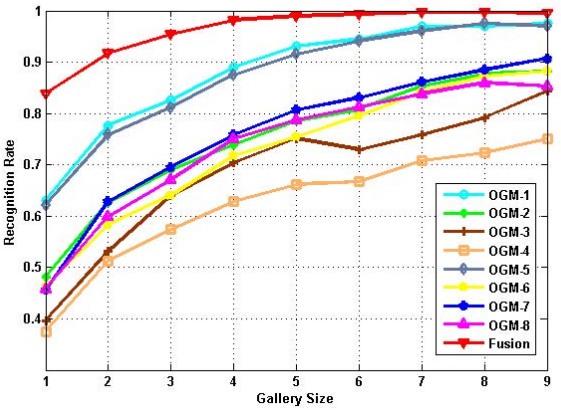

Fig. 6. Accuracy curves with respect to the gallery size of each subject

The cumulative match characteristic (CMC) curves with different numbers (from 1 to 9) of gallery samples of each subject are provided in Fig. 7.

5.3 The Comparison with the State of the Art

Table 2 compares the proposed method with the state of the art that evaluated their accuracies on the NCUT database. In [25], Wang et al. followed the way that firstly detects the vein region on each back of the hand and represents the region as a binary image, and then applies SIFT on the generated binary image for the matching step, originally introduced by Ladoux et al. [4] for palm vein recognition. we can see that if only using the vein region, their accuracy is only 78.68%, far behind the one achieved by the proposed method, showing that there indeed exists some useful information in the corium region that can contribute to the final result if described properly. Fig. 8 demonstrates an example of SIFT based keypoint matching using corresponding OGM pairs of two left hand images belonging to the same subject. It can be seen in Fig. 8 that due to the utilization of the OGMs, the details of the entire back of hand are highlighted, leading to a robust matching result. On the other hand, these matched keypoints of different

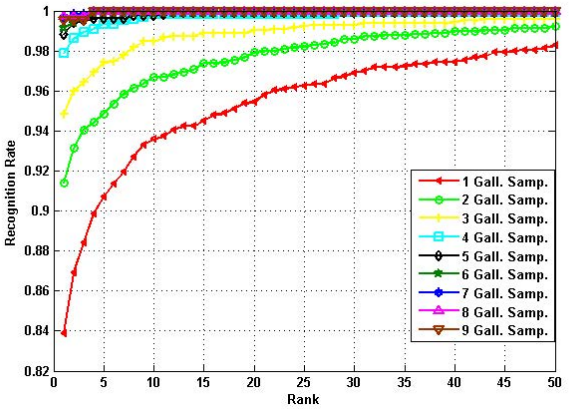

Fig. 7. Accuracy curves with respect to the number of gallery samples of each subject

OGM pairs are located in various positions, proving the fact once again that the similarity measurements of different orientations are complementary. Moreover, the matched keypoints distribute in the vein (marked in yellow) and surrounding corium (marked in red) area, indicating both the regions contribute to the final performance. Our accuracy is also slightly higher than the best one reported in [25] that was achieved by adopting the relationship of multiple gallery samples of each subject. In [14], Wang et al. employed the circular partition LBP (thus namely LCP), and achieved a recognition rate of 90.88% with 5 hand vein images in the gallery set and the remaining 5 ones used as probe. In our case, using the same protocol, much better performance is obtained.

Table 2. The Comparison with the state of the art on the NCUT dataset

Local feature	Class Num	Gallery/Probe	Results
OGM+SIFT	204	816/1224	**98.20%**
Binary+SIFT [25]	204	816/1224	78.68%
Best Binary+SIFT [25]	204	816/1224	97.95%
OGM+SIFT	204	1020/1020	**99.02%**
LCP [14]	204	1020/1020	90.88%

5.4 The Complementation of Left and Right Hands

Since vein patterns are different to some level for both hands of the same person [23], intuitively, the left and right hands of one person should possess complementary information for identification. In this experiment, we further investigate the answer to this problem by fusing the similarity measurement of each hand using the weighted sum rule as for combining the similarity of single OGM. We can see from Table 3 that the accuracy based on the fusion of both hands (in the

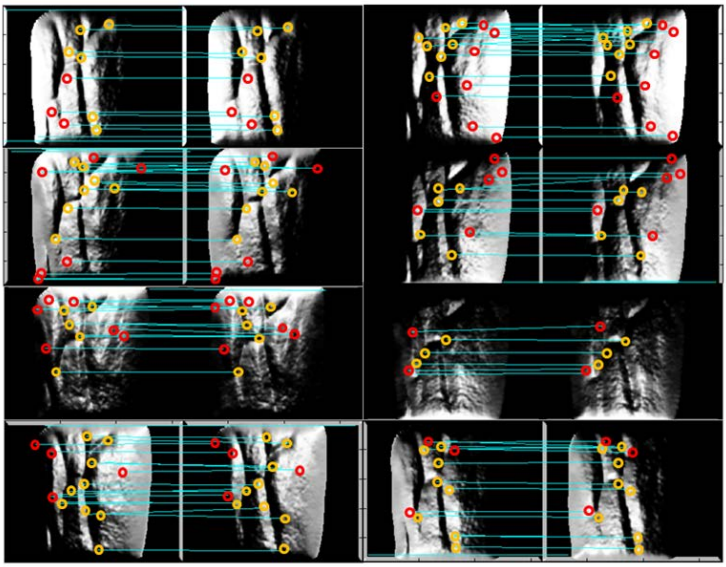

Fig. 8. A matching example using the corresponding OGM pairs of two left hands of the same subject. The left column from the top to the bottom: OGM1 to OGM4; while the right one with the same order: OGM5 to OGM8. The matched keypoints marked in yellow are located in the vein region; the red ones are in the corium area.

Table 3. The results of left hand only, right hand only, and their fusion using different numbers of gallery samples

Number of Gallery	Left Hands	Right Hands	Fusion of Both Hands
1	84.53%	84.31%	95.32%
2	92.28%	91.18%	97.92%
3	95.66%	94.96%	99.16%
4	97.55%	98.53%	100.00%
5	99.02%	99.02%	100.00%
6	99.22%	99.51%	100.00%
7	99.35%	100.00%	100.00%
8	99.51%	100.00%	100.00%
9	99.02%	100.00%	100.00%

3rd column) always outperforms that based on either of single hand, and we can achieve a rank-one recognition rate of 95.32% even using one enrolled hand vein sample. This fact clearly proves that left and right hands provide complementary cues for identifying persons.

6 Conclusions and Perspectives

In this paper, we presented the Oriented Gradient Maps (OGMs) as an effective representation of NIR back of the hand vein images to enhance the distinctiveness along with a local feature SIFT-based matching scheme to ameliorate the accuracy of back of the hand vein identification. Experimental results achieved on the NCUT databases clearly demonstrated the effectiveness of the proposed approach.

In future work, we will investigate other fusion strategies to combine different orientation scores for possible improvements on the final performance.

Acknowledgement. This work was supported in part by the National Basic Research Program of China under grant 2010CB327902; the National Natural Science Foundation of China (No. 61273263, No. 61202237, No.61271368); and the Fundamental Research Funds for the Central Universities.

References

1. Kumar, A., Hanmandlu, M., Gupta, H.M.: Online biometric authentication using hand vein patterns. In: IEEE Symposium on Computational Intelligence for Security and Defence Applications (2009)
2. MacGregor, P., Welford, R.: Imaging for security and personnel identification. Advanced Imaging 6, 52–56 (1991)
3. Malki, S., Spaanenburg, L.: Hand veins feature extraction using dt-cnns. In: SPIE International Symposium on Microtechnologies for the New Millennium, vol. 6590 (2007)
4. Ladoux, P., Rosenberger, C., Dorizzi, B.: Palm vein verification system based on sift matching. In: IEEE International Conference on Biometrics (2009)
5. Lin, C., Fan, K.: Biometric verification using thermal images of palm-dorsa vein patterns. IEEE Transactions on Circuits and Systems for Video Technology 14, 199–213 (2004)
6. Zhao, S., Wang, Y., Wang, Y.: Biometric identification based on low quality hand vein pattern images. In: IEEE International Conference on Machine Learning and Cybernetics (2008)
7. Kumar, A., Prathyusha, K.: Personal authentication using hand vein triangulation and knuckle shape. IEEE Transactions on Image Processing 18, 2127–2136 (2009)
8. Miura, N., Nagasaka, A., Miyatake, T.: Feature extraction of finger-vein pattern based on repeated line tracking and its application to personal identification. Machine Vision and Applications 15, 194–203 (2004)
9. Cross, J., Smith, C.: Thermographic imaging of the subcutaneous vascular network of the back of the hand for biometric identification. In: IEEE International Carnahan Conference on Security Technology (1995)
10. Wang, K., Yuan, Y., Zhang, Z., Zhuang, D.: Hand vein recognition based on multi-supplemental features of multi-classifier fusion decision. In: IEEE International Conference on Mechatronics and Automation (2006)
11. Huang, D., Ben Soltana, W., Ardabilian, M., Wang, Y., Chen, L.: Textured 3d face recognition using biological vision-based facial representation and optimized weighted sum fusion. In: IEEE International Conference on Computer Vision and Pattern Recognition Workshop on Biometrics (2011)

12. Wang, L., Leedham, G.: Near- and far-infrared imaging for vein pattern biometrics. In: IEEE International Conference on Advanced Video and Signal-based Surveillance (2006)
13. Zhao, S., Wang, Y., Wang, Y.: Extracting hand vein patterns from low-quality images: a new biometric technique using low-cost devices. In: IEEE International Conference on Image and Graphics (2007)
14. Wang, Y., Li, K., Cui, J., Shark, L., Varley, M.: Study of hand-dorsa vein recognition. In: IEEE International Conference on Intelligent Computing (2007)
15. Edelman, S., Intrator, N., Poggio, T.: Complex cells and object recognition. Unpublished manuscript (1997), http://kybele.psych.cornell.edu/~edelman/archive.html
16. Gabor, D.: Theory of communications. Journal of the Institute of Electrical Engineers 93, 429–457 (1946)
17. Tola, E., Lepetit, V., Fua, P.: Daisy: an efficient dense descriptor applied to wide baseline stereo. IEEE Transactions on Pattern Analysis and Machine Intelligence 32, 815–830 (2010)
18. Marcelja, S.: Mathematical description of the responses of simple cortical cells. Journal of the Optical Society of America 70, 1297–1300 (1980)
19. Daugman, J.: High confidence visual recognition of persons by a test of statistical independence. IEEE Transactions on Pattern Analysis and Machine Intelligence 15, 1148–1161 (1993)
20. Liu, C., Wechsler, H.: Gabor feature based classification using the enhanced fisher linear discriminant model for face recognition. IEEE Transactions on Image Processing 11, 467–476 (2002)
21. Lowe, D.G.: Distinctive image features from scale-invariant key-points. International Journal of Computer Vision 60, 91–110 (2004)
22. Mian, A.S., Bennamoun, M., Owens, R.: Keypoint detection and local feature matching for textured 3d face recognition. International Journal of Computer Vision 79, 1–12 (2008)
23. Badawi, A.M.: Hand vein biometric verification prototype: A testing performance and patterns similarity. In: International Conference on Image Processing, Computer Vision and Pattern Recognition, pp. 3–9 (2006)
24. Chen, L., Huang, D., Chiheb, H., Ben Amar, C.: Increasing the distinctiveness of hand vein images by oriented gradient maps. In: International Conference of the Special Interest Group on Biometrics and Electronic Signatures (2011)
25. Wang, Y., Fan, Y., Liao, W., Li, K., Shark, L., Varley, M.: Hand vein recognition based on multiple keypoints sets. In: International Conference on Biometrics (2012)